RSC Advances

ROYAL SOCIETY OF CHEMISTRY

www.rsc.org/advances

Antiproliferative activity and conversion of tachyzoite to bradyzoite of *Toxoplasma gondii* promoted by new zinc complexes containing sulfadiazine

Luana C. Batista [a], Fernanda S. de Souza [b], Vagner M. de Assis [a], Sérgio H. Seabra [c], Adailton J. Bortoluzzi [d], Magdalena N. Rennó [e], Adolfo Horn Jr [a], Renato A. DaMatta [b], Christiane Fernandes [a,*]

[a]*Laboratório de Ciências Químicas, Universidade Estadual do Norte Fluminense Darcy Ribeiro, 28013-602 Campos dos Goytacazes, RJ, Brazil.*

[b]*Laboratório de Biologia Celular e Tecidual, Universidade Estadual do Norte Fluminense Darcy Ribeiro, 28013-602 Campos dos Goytacazes, RJ, Brazil.*

[c]*Laboratório de Tecnologia em Cultura de Células, Centro Universitário Estadual da Zona Oeste, 23070-200 Rio de Janeiro, RJ, Brazil.*

[d]*Departamento de Química, Universidade Federal de Santa Catarina, 88040-900 Florianópolis, SC, Brazil.*

[e]*Laboratório de Modelagem Molecular e Pesquisa em Ciências Farmacêuticas (LAMCIFAR), Núcleo em Ecologia e Desenvolvimento Sócio-Ambiental de Macaé (NUPEM), Universidade Federal do Rio de Janeiro Campus Macaé Professor Aloísio Teixeira, 27965-045,Macaé, RJ, Brazil.*

Corresponding author. Tel.: +55 22 2739 7213; fax: +55 22 2739 7046.

E-mail address: chrisf@uenf.br (C. Fernandes)

Abstract

Here we describe the synthesis and biological effect against *Toxoplasma gondii* of two new zinc complexes containing sulfadiazine:[(SDZ)Zn(μ-BPA)$_2$Zn(SDZ)] **1** and [Zn(SDZ)(HSDZ)(Cl)(OH$_2$)] **2**, where SDZ is the anion sulfadizine. The complexes were characterized by elemental analysis, IR, ^{1}H NMR, UV-Vis, electrospray ionization ESI(+)-MS and tandem mass spectrometry ESI(+)-MS/MS. X-ray diffraction studies were performed for complex **1** revealing the presence of sulfadizine molecules coordinated to the metal center, resulting in a dinuclear complex. The cytotoxic effects of both complexes on *T. gondii* infecting LLC-MK2 host cells are presented and indicate that both reduced the growth of *T. gondii* in this cell. After 48 h of treatment, both compounds induced the formation of pseudocysts confirmed by fluorescence microscopy performed with *Dolichos biflorus* lectin, a cystic wall marker. Pseudocysts were not observed in untreated cells or after treatment with NaSDZ alone. These results suggest the effect of the metal and the ligand on the anti-toxoplasma activity. *In silico* molecular pharmacokinetics studies indicate poor permeability and oral bioavailability exhibited by complex **1**. As complex **1** presents better antitoxoplasma activity than SDZ we suggest that complex **1** could be acting by a distinct mode of action than SDZ which until now is unclear.

Introduction

Toxoplasma gondii is an obligate intracellular protozoan parasite that resides in a parasitophorous vacuole and infects over a billion humans worldwide.[1] It causes severe disease in individuals with compromised immune system, such as HIV patients and immunosuppressed organ transplanted patient. Under such conditions, *T. gondii* can result in life-threatening toxoplasmosis with Toxoplasma encephalitis and other complications (i.a. necrotic lesions within the central nervous system or retinochoroiditis).[2] Women infected with *T. gondii* for the first time during pregnancy will pass the parasite on to the fetus. Congenital toxoplasmosis may result in serious neurological and ophthalmic damage to the fetus or even like, especially in the first three months of pregnancy, spontaneous abortion. Furthermore, reactivation of undiagnosed congenital toxoplasmosis can lead to ocular toxoplasmosis later in life, in many cases causing blindness.[3] For most of the healthy individuals *T. gondii* does not cause severe disease, however, strains that have caused severe toxoplasmosis in healthy immuncompetent adults have been identified.[4] Infections can last for the life of the individual, and to date all available drugs act primarily against tachyzoites and do not eradicate bradyzoites in tissue cysts within host cells, furthermore they are not effective in eliminating the parasite located in cells of the central nervous system.

In spite of the severe consequences of toxoplasmosis, the therapy for this disease has not been changed in the last years. The current treatment involves the use of synergistic combinations of pyrimethamine, which inhibits the enzymatic activity of dihydrofolate reductase, and sulfonamides such as trimethoprim-sulfamethoxazole or sulfadiazine (SDZ or 2-sulphanilamidopyrimidine), whose target is dihydropteroate synthetase (IC_{50} 600-700 mg/L)[5]; patients receive also folinic acid supplementation.[6,7] The efficacy of this regime is limited, requiring the administration of large amounts of

drugs. Side effects include hypersensitivity, haematological toxicity, teratogenicity, allergic reactions, bone marrow suppression, and the development of resistance.[8]

The antimicrobial activity of sulfadiazine is thought to come from the structural resemblance between sulphanilamide group and p-amino benzoic acid where the sulfa drug mimics this metabolite and blocks folic acid synthesis in bacteria, thereby causing cell death. Folic acid is required for the biosynthesis of purines, pyrimidines and certain amino acids.[9]

Recently, Felix and co-workers described the use of trimethoprim-sulfamethoxazole (160 mg–800 mg) for 45 days, to threat active toxoplasma retinochoroiditis.[10] An alternative treatment is pyrimethamine in conjunction with clindamycin, spiramycin or atovaquone, but each of these drugs possess their own limitations.[11] Thus, limited efficacy and side effects of existing drugs together with severe damage caused by *T. gondii* infection clearly indicates the need for the development of new non-toxic, well-tolerated, and more efficacious therapeutic agents for controlling and curing toxoplasmosis. Reis and co-workers reported the use of atovaquone in toxoplasma retinochoroiditis. This drug is FDA and EMEA approved for the treatment of pneumocystis infections. They reported two cases in which the treatment was based on the ingestion of 750 mg, twice, for 21 days. No side effects have been reported and after this period no Toxoplasma activity was observed.[12]

Unfortunately, there is no large scale trials on the efficacy of drugs used to treat toxoplasmosis.[13] Some organic compounds have been investigated aiming to get insights about the mechanism of death and to identify new chemical scaffolds that could form the basis for new therapeutics.[14] In 2011, Boyle and co-workers investigated 17 candidate compounds, and identified one organic molecule with potent antiparasitic activity. The compound has an IC_{50} of 2 nM, and the mode of killing seems to involve

the destruction of *T. gondii* membrane integrity, which leads to the lysis of the parasites.[15]

Our research group has been developing complexes with interesting biological activity.[16-19] Our studies indicate that the ligands exert a relevant effect on the biological activity. Recently, we reported the cytotoxic effect on *T. gondii* of a dinuclear iron(III) complex $[Fe(HPClNOL)(SO_4)]_2$-μ-oxo, which induces cyst formation, reduction of superoxide dismutase and catalase activities of the parasite, disturbs the redox equilibrium of *T. gondii* resulting in cystogenesis and parasite death.[20] Unfortunately, the reactions between the complex $[Fe(HPClNOL)(SO_4)]_2$-μ-oxo and NaSDZ were unsuccessful, due the hindrance of the ligand HPClNOL. Therefore, we decided to investigate the reaction between coordination compounds containing smaller ligands, like HBPA, in order to attach SDZ molecule to them. This strategy aims to improve the solubility of SDZ and to increase the intake by the cells. In this sense, complex **1** was obtained by the reaction between $[Zn(HBPA)Cl_2]$ [21] and NaSDZ and complex **2** was obtained by the reaction between $ZnCl_2$ and NaSDZ, in order to investigate their *in vitro* anti-toxoplasma effect. In addition, zinc can improve the immune defense due to its catalytic and regulatory functions, thus, enhancing resistance to infections.[22-25.]

Results and discussion

Chemistry

In our attempt to generate compounds with two interesting features (i.e. compounds containing zinc, which is associated with adequate immunological system activity, and sulfadiazine, as well) we have prepared two new zinc complexes. Complex **(1)** is a dinuclear zinc complex containing two molecules of the ligand BPA^- and two SDZ^-, while complex **(2)** was prepared in the absence of the ligand HBPA, resulting in

a complex with formulae [Zn(SDZ)(HSDZ)(Cl)(OH_2)], which contains one protonated (HSDZ) and one deprotonated sulfadiazine molecule (SDZ^-) coordinated to the zinc center. Our aim was to evaluate effect of the complexation of SDZ^- to zinc on the anti-toxoplasma activity, since NaSDZ is traditionally employed in the treatment of toxoplasma. Furthermore, we intend to investigate the effect of the ligand HBPA on the anti-toxoplasma activity. The complexes were easily obtained as crystalline and microcrystalline white solids directly from the mother solution or after recrystallization in suitable solvents, like acetonitrile/water (1:1) under heating. The complexes are very stable in air. They are remarkably soluble in polar aprotic solvents such as DMF, DMSO; slightly soluble in ethanol, methanol and chloroform and insoluble in water. The low conductivity values observed for both complexes suggest that they are non-electrolyte and indicate that the arrangement observed in solid state is the same in solution. Scheme 1 presents the proposed structures based on X-ray data for compound **1** and spectroscopic characterization for compound **2.**

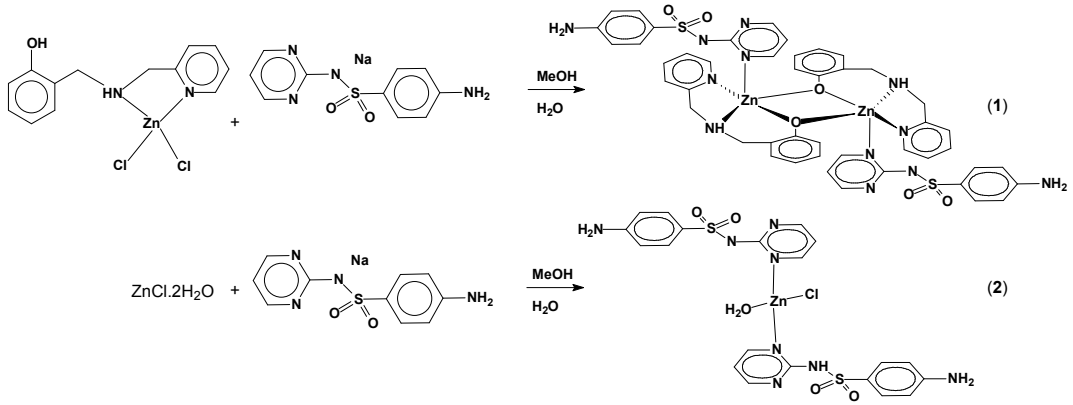

Scheme 1. Scheme for the synthesis of the complexes **1** and **2**.

Description of the structure of complex **1**

Recently, we reported the X-ray crystal structure for the starting complex [Zn(HBPA)Cl_2] where HBPA is (2-hydroxybenzyl-2-pyridylmethyl)amine. This

complex is a mononuclear species and the zinc ion presents a tetrahedral geometry. It is coordinated by two nitrogen atoms from the ligand HBPA and two chloro ligands. The phenol group present in the ligand HBPA remains protonated and uncoordinated.[21] After the reaction with NaSDZ, a new zinc complex was obtained showing the presence of the SDZ molecule coordinated to the zinc. A perspective view of compound **1** is displayed in Figure 1. Bond lengths and angles for compound **1** are listed in Table 1 (supplementary material). The data reveals that complex **1** consists of a neutral dinuclear zinc complex. Each zinc is coordinated to three nitrogen (amine, pyridine and to the pyrimidine ring N atom of sulfadiazine molecule (SDZ^-)) and two oxygen (phenolate) atoms, resulting in the same coordination for both metal centers. To balance the charge on Zn centers, each amido group of SDZ is deprotonated (SDZ^-). The zinc ions are pentacoordinated and the polyhedron around the Zinc ion can best described as slightly distorted trigonal-bipyramidal geometry. The metal centers Zn1 and Zn2 are linked by two ligand-derived phenolates (O10 and O30), these bond lengths are essentially equivalent (Zn1-O10= 2.0338(15), Zn1-O30= 2.0592(15), Zn2-O10= 2.0518(15) and Zn2-O30= 2.0360(15) Å), matching observations in the literature.[26] The Zn1$\cdots$ Zn2 distance is 3.1698(3)Å, which is similar to previously reported values for phenolate–dizinc compounds (3.16–3.02 Å).[26] The Zn1–O10–Zn2 and Zn1–O30–Zn2 bridging angles are 101.77(7) and 101.43(6), respectively, which are smaller than those found for similarly coordinated-phenolate zinc(II) dimers containing one cresolic bridge (119.36(11)º)[27] and similar to those found for similarly coordinated-phenolate Zn(II) dimers containing two phenolate bridges.[28] However, these bridging angles are bigger than those found for a nickel(II) dimer, previously reported by us in 2006, which was obtained with H_2BPClNOL ligand, which presents the HBPA unit in its structure.[29]

In 1983, N. C. Baenziger and co-workers reported the X-ray crystal structure of a mononuclear zinc complex containing SDZ^-, $[Zn(SDZ)_2(NH_3)_2]$, in which the zinc is coordinated to two sulfadiazine molecules and two ammonia molecules, resulting in a distorted tetrahedrally center. Different N atoms from the sulfadiazine molecule are involved in the coordination to the Zn atom. One sulfadiazine molecule is coordinated by the imido N atom and the other is coordinated by the pyrimidine ring N atom.[30] In 2001, X. -Z. You and co-workers reported the X-ray crystal structure of $[Zn(SDZ)_2]$ obtained by the solvothermal reaction condition between $Zn(OAc)_2.2H_2O$ and NaSDZ, in water/ethanol. The SDZ moiety acts as a tridentate bridging ligand through the nitrogen atom of the pyrimidine ring, the imido nitrogen and the oxygen of the sulfonyl group connect two Zn atoms, resulting in the formation of a one-dimensional polymeric $[Zn(SDZ)_2]$ chain. In addition, one oxygen atom of the sulfonyl group and the other nitrogen atom of the pyrimidine ring in the same ligand are chelated to the same zinc atom to form a stable six-membered ring. The bond length Zn–Nsulfonamido (1.967(3) Å) is slightly shorter than Zn–Npyrimidine (2.017(3) or 2.060(2) Å), probably due to the deprotonated amido N atom being negatively charged and able to bind the Zn center ions easier than the N atom of the pyrimidine ring.[31] For complex **1**, the bond length Zn–Npyrimidine are (2.0813(19) and 2.0268(18) Å), slightly longer than reported by X.-Z. You and co-workers.[31]

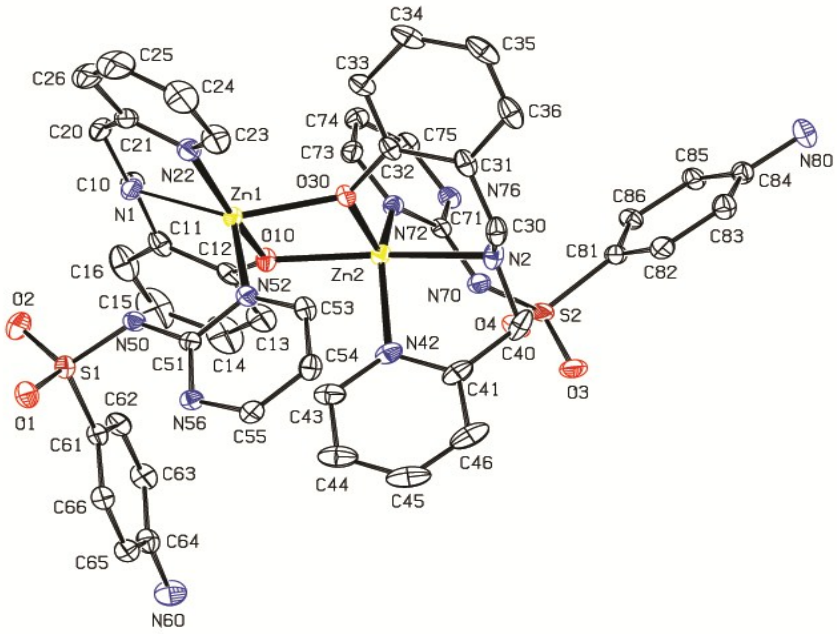

Fig. 1 View of the *ORTEP* projection for compound **(1)** and the corresponding residue labeling scheme. Ellipsoids are shown at the 40% probability level. Hydrogen atoms were omitted for clarity.

IR, ESI(+)-MS, ESI(+)-MS/MS and ^{1}H NMR for complexes **1** and **2**

The IR spectra of complexes **1** and **2** were analyzed in comparison with their precursor molecules. The IR spectrum of NaSDZ, reported by J. Guo and co-workers reflects that the $–NH_2$ vibration absorption peaks are at 3425 and 3560 cm^{-1}. The symmetric and asymmetric vibration absorption peaks of $–SO_2–$ can be observed at 1322 and 1154 cm^{-1}. These are the main bands present in the IR spectrum of NaSDZ.[32] The coordination of SDZ molecule to the zinc center results in shifts for the main vibration absorptions, indicating the coordination of SDZ to the zinc center in both complexes. Furthermore, the strong bands related to ν_a and ν_s of the (SO_2–N) moiety at 1322 and 1154 cm^{-1} in sodium sulfadiazine show important changes upon

complexation. For complexes **1** and **2**, the absorptions related to to ν_a and ν_s of the (SO_2–N) moiety were observed at 1341 and 1157 cm^{-1} and at 1328 and 1157 cm^{-1}, respectively and the absorption peaks related to $–NH_2$ were observed at 3356 and 3423 cm-^{1} for complex **1** and at 3354 and 3424 cm^{-1} for complex **2**.

ESI(+)-MS and ESI(+)-MS/MS of complexes **1** and **2** present a characteristic set of isotopologue ions due mainly the presence of metal atoms. For compound **1**, ESI(+)-MS data indicate the presence of six cations in MeOH:H_2O (1:1) solution (peaks at *m/z* 491, 527, 565, 601, 741, 807 and 843). The proposal for each peak, based on isotopic distribution is: $[Zn(HBPA)(BPA)]^+$ (*m/z* 491), $[Zn(HBPA)(SDZ)]^+$ (*m/z* 527), $[Zn(HBPA)(Cl)(HSDZ)]^+$ (*m/z* 565), $[Zn(HBPA)(H_2O)_2(Cl)(HSDZ)]^+$ (*m/z* 601), $[Zn(HBPA)_2(SDZ)]^+$ (*m/z* 741), $[Zn(SDZ)$-$(\mu$-$BPA)_2$-$Zn]^+$ (*m/z* 807) and $[Zn(HSDZ)$-$(\mu$-$BPA)_2$-$Zn(Cl)]^+$ (*m/z* 843). MS/MS data for the species with *m/z* 843 yields the cation with *m/z* 491, by the loss of a neutral [Zn(SDZ)Cl], and the cation with *m/z* 527 by the loss of a neutral [Zn(SDZ)], with reduction to Zn(I). For complex **2**, ESI(+)-MS data indicate the presence of six cations in MeOH:H_2O (1:1) solution (peaks at *m/z* 251, 273, 289, 563, 581 and 813). The proposal for each peak, based on isotopic distribution is: $[HSDZ]^+$ (*m/z* 251), $[HSDZ$-$Na]^+$ (*m/z* 273), $[Na$-SDZ-$OH]^+$ (*m/z* 289), $[Zn(HSDZ)(SDZ)]^+$ (*m/z* 563), $[Zn(HSDZ)(SDZ)(H_2O)]^+$ (*m/z* 581), and $[Zn(HSDZ)_2(SDZ)]^+$ (*m/z* 813). MS/MS data for the species with *m/z* 813 yields the cation with *m/z* 572 ($[Zn(HSDZ)(SDZ)(OH)]^+$) which generates the peak with *m/z* 273 ($[HSDZ$-$Na]^+$), by the loss of a neutral [(HSDZ)(OH)(CH_3OH)] (*m/z* 299). The high intensity for the peak at *m/z* 563 indicates high stability of this cation in solution, in good agreement with our proposal based on elemental analysis and IR (see Figure 2).

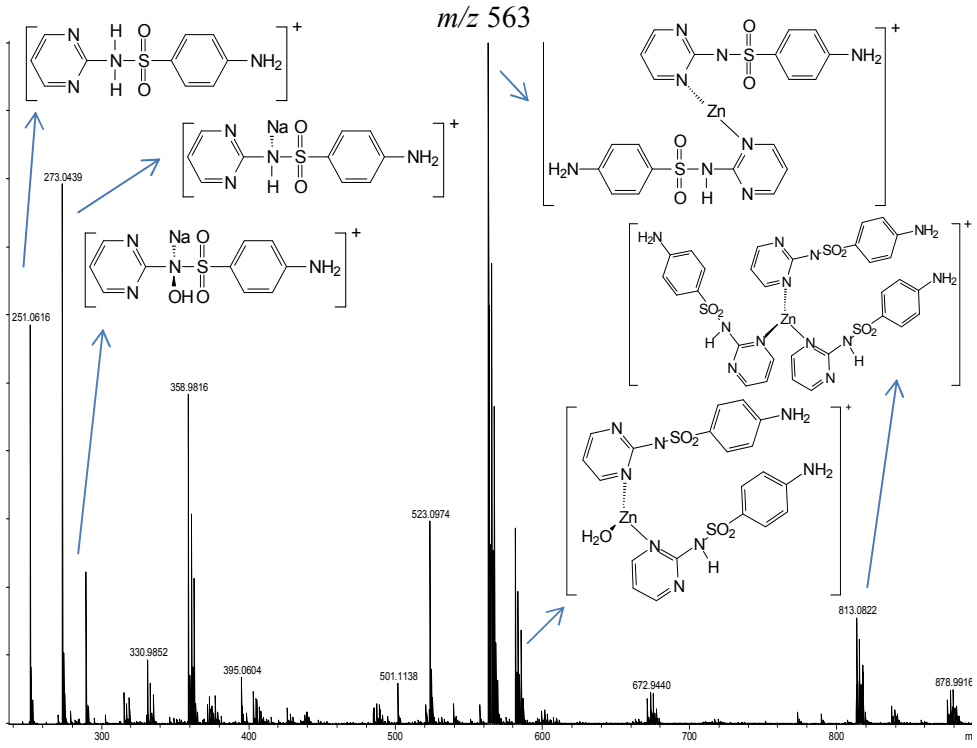

Fig. 2 ESI(+)-MS spectrum of complex **2**, in H_2O/MeOH (1:1).

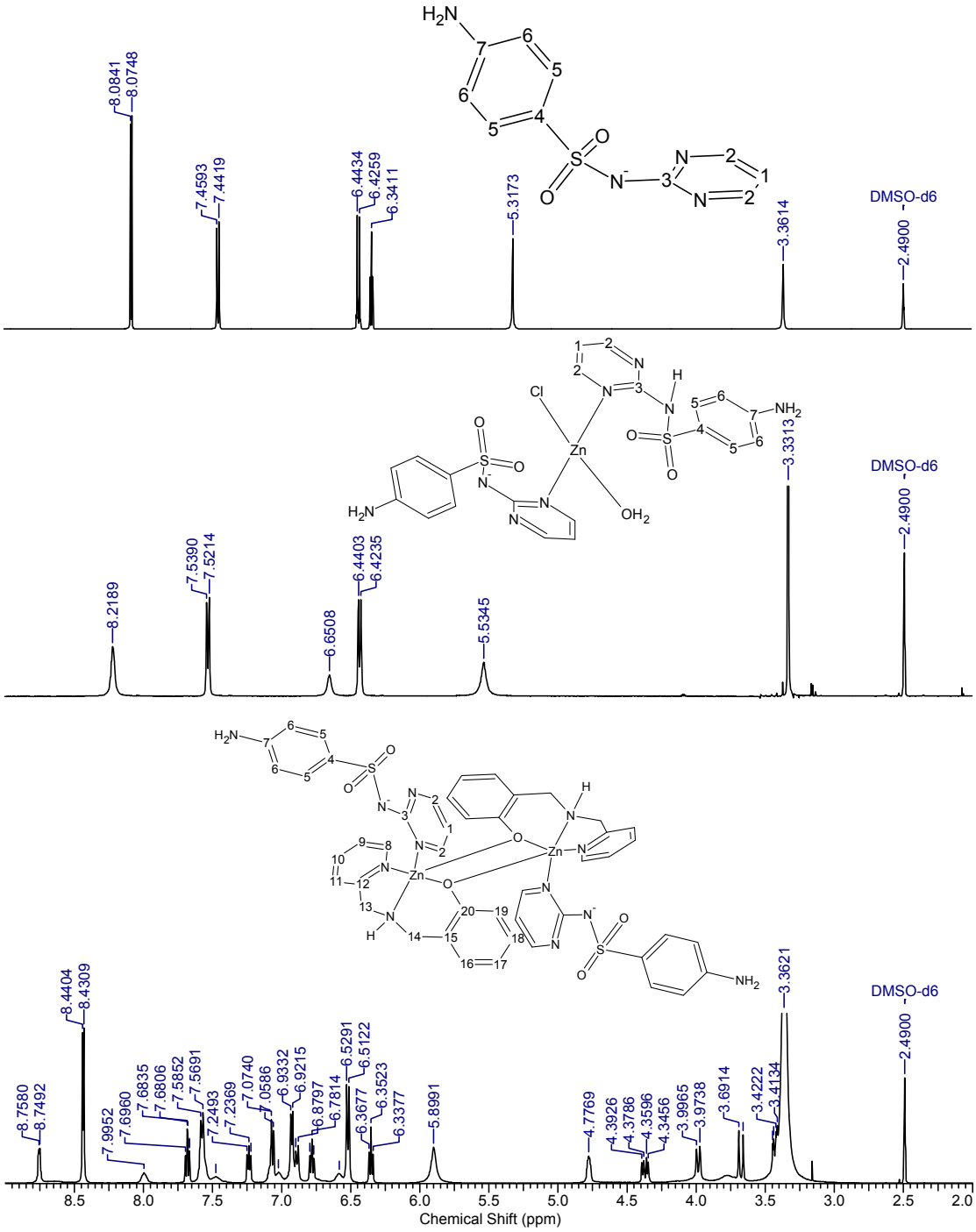

Fig 3. ^{1}H NMR spectra (DMSO-d_6, 500 MHz) of sodium sulfadiazine (top), complex **2** (middle) and complex **1** (bottom).

The ^{1}H NMR spectrum of the sulfadiazine sodium salt is similar to that reported in the literature (Figure 3).[33] The hydrogen atoms from the pyrimidine ring (C1 and C2) are observed as a doublet (8.08 ppm, 2 H, J = 4.7 Hz) and a triplet (6.34 ppm, 1 H, J = 4.7 Hz), respectively. The hydrogen atoms associated with the aniline ring are observed as doublets at 7.45 (C5) and 6.43 (C6) ppm (J = 7 Hz). The NH_2 protons are at 5.32 ppm (broad singlet). The spectrum of complex **(2)**, obtained by the reaction between $ZnCl_2$ and sodium sulfadiazine, is different from the SDZ^- sodium salt. The first difference was that almost all the signals underwent a downfield shift, except the signal associated with the hydrogen at *orto* position to NH_2 group, indicating a change in the electronic density around the whole molecule. This change was greater for the hydrogen atom located at C1 (Δ = + 0.31 ppm) and for the NH_2 (Δ +0.21 ppm), which reflects the coordination of SDZ molecule to the zinc ion. Although the shift of the signal associated with the NH_2 group indicates a significant change in its electron density, it is not possible to state that this group is interacting with the metal ion since the two zinc complexes containing sulfadiazine reported up to now do not show this interaction with the zinc center.[30,31] Furthermore, for the complex $[Hg(SDZ)_2(DMF)_2]$, the NH_2 protons are observed at 5.92 ppm and its molecular structure solved by x-ray diffraction reveals that this group is not interacting with the metal center.[34]

The hydrogen atoms from the aniline unit appear at 6.43 and 7.53 ppm in complex **1**, while in the NaSDZ, they were observed at 6.43 and 7.45, respectivelly. Significant changes occurred with the signals of the hydrogen atoms associated with the piperazine ring. The hydrogen atom attached to C1 appears as a triple at 6.34 ppm in the NaSDZ spectrum. On the other hand, in compound **2,** it appears as a broad singlet at 6.65 ppm. The hydrogen atoms at C2 position of the piperazine unit were shifted to 8.22 ppm (broad singlet), while in the free ligand they were at 8.08 ppm (doublet).

Comparing the NMR of the NaSDZ and complex **2**, the shift in the signal associated with the hydrogen from the piperazine and the NH_2 groups, support the proposal that SDZ is possibly interacting with the zinc ion through the piperazine and sulfonamide units. Hydrogen atoms associated with the imido group were not observed. However, the elemental analysis indicates that the imido groups should be protonated, due to the presence of a chloride and hydroxide ions in the composition. The lack of signal in the NMR spectrum related to the imido hydrogen can be due to the exchange of the imido hydrogen with deuterium from the solvent.

In the ^{1}H NMR spectrum of complex **1**, the signals related with the SDZ^- molecule show features different from those observed in NaSDZ and in complex **2**. The H-H COSY spectrum shows that the hydrogen atoms from the pyrimidine unit, which appeared as broad singlets in the compound **2**, now appear as two doublets at 8.43 ppm (C2, 4 H, J = 4.8 Hz) and 6.92 ppm (C1, 2 H, 8.07 Hz). The hydrogen atoms related to aniline ring are located at 7.57 ppm (C5, brd, 4 H, J = 8.07 Hz) and at 6.52 ppm (C6, d, 4 H, J = 8.4 Hz). Concerning the aromatic hydrogen from the HBPA molecule, the hydrogen atom attached to C8, C9, C10 and C11 are observed, respectively, at 8.75 (d, 2H, J = 4.41 Hz), 7.24 (t, 2H, J = 6.24 Hz), 7.68 (dt, 2 H, J = 1.5 and 7.70 Hz) and 7.06 ppm (d, 2 H, J = 7.71 Hz). Signals associated with the phenolate rings are observed at 6.35 (C17, t, J = 7.3 Hz), 7.78 (C18, t, J = 7.3 Hz), 6.88 (C19, d, J = 8.1 Hz) and 6.92 (C16, d, J = 7.3 Hz). The NH_2 protons appear at 5.89 ppm. The aliphatic hydrogen atoms (C13 and C14) were split in four set of signals. The hydrogens atoms attached to C14 appear at 4.36 ppm (dd, 2 H, J = 7.0 and 16 Hz) and 3.67 (d, 2H, J = 16 Hz), while the hydrogen bound to C13 are at 3.98 (d, 2 H, J = 11.4 Hz) and 3.43 ppm (dd, 2 H, J = 4.4 and 12.3 Hz). There is yet a broad signal at 4.77 ppm, which is attributed to N-H proton, since the H-H COSY spectrum shows that it is coupling which the hydrogen

atoms attached to C13 and C14. In the aromatic range (6 – 9 ppm) it is possible yet to see some broad signals with low intensity at 6.58, 7.02, 7.47 and 7.99 ppm. Again, the H-H COSY spectrum shows that the signal at 7.99 is coupling with the signal at 7.47, while the signal at 7.02 is coupling with the signal at 6.58. The pattern suggests that these signals are related with the SDZ^- molecule, indicating that about 20 % of the SDZ molecules are in a different conformation in comparison to the signals presented above.

In vitro antitoxoplasma activity

The host cell viability data of the complexes are shown in Fig. 4. Both compounds were non-toxic to the host cells. For complex **1** until the concentration of 100 μmol L^{-1} the cell viability was above 95%. This data reveals that at a concentration 20 times higher than the maximum concentration used in the anti-proliferative assays (5 μmol L^{-1}), the complex was non-toxic and did not interfere in the growth of LLC-MK2 cells.

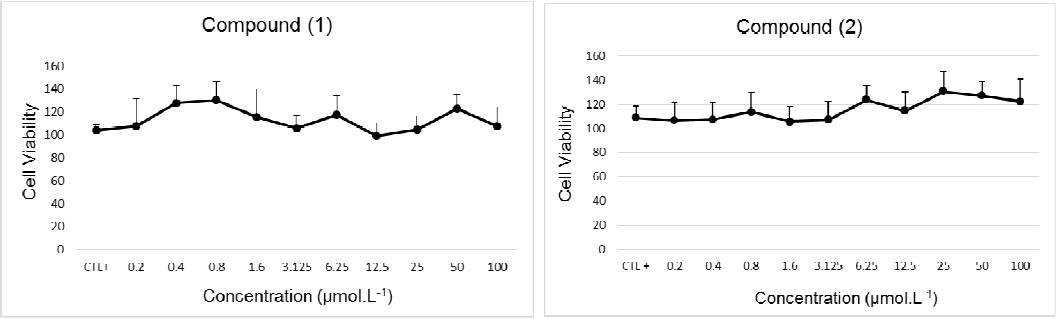

Fig. 4 Cell viability of LLC-MK2 after treatment for 24 h with complexes **1** and **2** at the indicated concentrations by the MTT assay. Representative experiment of three repetitions performed in triplicate. No significant differences were found.

Complexes **1** and **2** reduced the growth of *T. gondii* in LLC-MK2 cells (Figure 5). Comparing with control and with NaSDZ after 24 h of treatment, complex **1** presented the highest anti-toxoplasma effect. At 24 h in the concentration of 0.5 μmol L^{-1}, this complex reduced *T. gondii* growth in 53% compared to the control and 36% compared to SDZ alone. For 48 h of treatment (Figure 5), the reduction was 51% compared to the control and 23% in relation to SDZ. After 24 h, complex **2** did not change the growth rates of *T. gondii* (Figure 5). However, after 48 h of treatment this complex was active reducing in 58% the growth of *T. gondii* in relation to the control and 34% when compared with NaSDZ at concentration of 5 μmol L^{-1}. These results indicate that both complexes **1** and **2** were more effective than the treatment employing pure NaSDZ. Although both complexes showed similar activity after 48 h, complex **1** was better for the first 24 h of treatment. There was no significant difference among the concentrations employed. It may be suggested that the difference in the activities of complexes **1**, **2** and SDZ at 24 and 48 h is related with the structure of these complexes and the results point out the relevance of the ligand HBPA for the anti-toxoplasma activity.

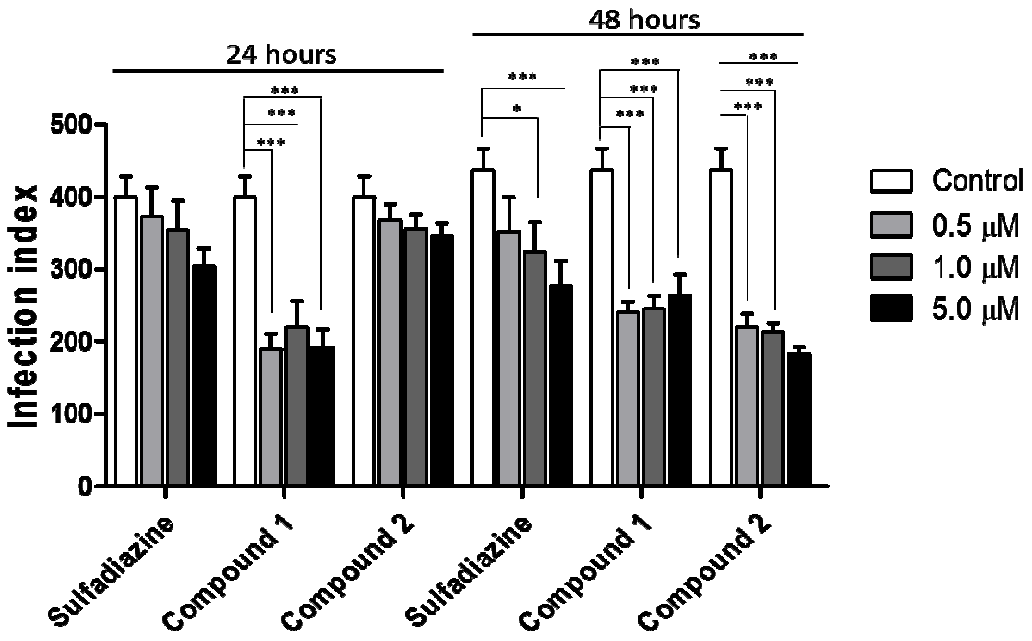

Fig. 5 *Toxoplasma gondii* growth in LLC-MK_2 cells treated for 24 and 48 h with different concentrations of complex **1**, **2** and sulfadiazine. Untreated cells are the control. Representative experiment of three repetitions performed in triplicate. Significant difference with *** $P < 0.001$ and * $P < 0.05$.

The evaluation of the antiproliferative activity was performed after staining treated cells with Giemsa. To calculate the infection index, parasites inside the host cells forming rosettes or isolated in the parasitophorous vacuoles were counted (Figure 6A and B). After 48 h of incubation with the complexes **1** and **2**, most of the parasites were clusters and the edges of the parasitophorous vacuoles were highly stained suggesting the formation of pseudocysts (Figure 6 - C and D). The presence of these pseudocysts suggests that both compounds promoted the conversion of tachyzoites to bradyzoites. Independently of the culture time, this structure was not observed in cells treated with the lowest concentration of complexes **1** and **2** (not shown) or with SDZ (Figure 6B).

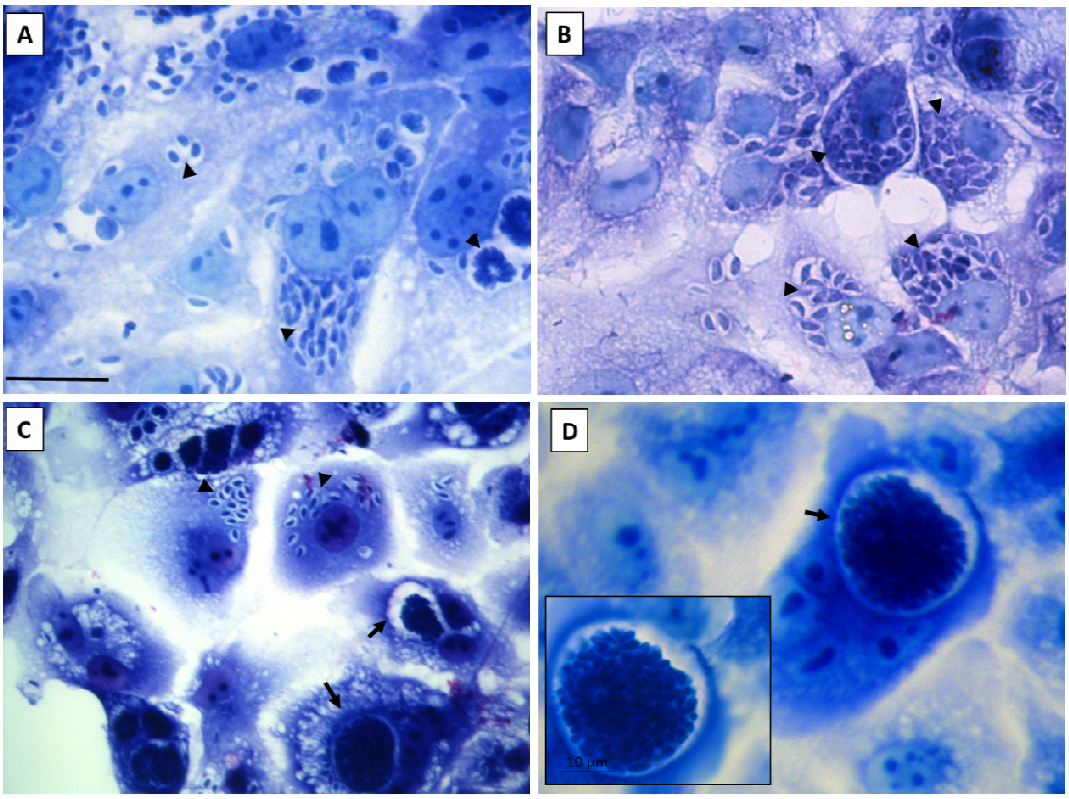

Fig. 6 Representative images of Giemsa stained LLC-MK_2 cells infected with *Toxoplasma gondii* for 48 h of treated or not with complexes **1**, **2** or sulfadiazine. A) Non-treated infected cells. B) Infected cells treated with sulfadiazine (0.5 µmol L^{-1}). C) Infected cells treated with compound **1** (1 µmol L^{-1}). D) Infected cells treated with compound **2** (1 µmol L^{-1}); inset show parasite structure at different focus then the primary image. Structures similar to tissue cists (arrows) and tachyzoites (arrowheads) can be seen. Images are from three independent experiments. Bar = 20 µm.

The formation of pseudocysts was confirmed by fluorescence microscopy analysis performed with a specific marker of the cystic wall (DBA lectin) of the parasite after 48 h of treatment. DBA labeling (green fluorescence) was not observed in the control (Figure 7A) or after treatment with SDZ (Figure 7E). Untreated control cells presented a large number of parasites occupying most of the host cell cytoplasm (Figure 7 - A to D). Tachyzoites were organized in rosettes even after 48 h of infection (Figure 7D). In cells treated with 5 µmol L^{-1} of SDZ many parasites were also seen in the cell

cytoplasm (Figure 7 – E to H). However, after treatment with complexes **1** (Figure 7 – I to P) and **2** (Figure 7 – Q to X), in concentrations of 0.5 μmol L^{-1} and 5.0 μmol L^{-1}, respectively, DBA labeling was positive (Figure 7 - I, M, Q, U) indicating formation of the pseudocysts.[35] Some studies have already explored the morphological features associated with *T. gondii* death. Ling and co-workers showed that this intracellular mechanisms used by primed macrophage to destroy *T. gondii* occurs frequently at early stages of infection, and is characterized by changes of the parasitophorous vacuole membrane and parasite disorganization, which lead to autophagic processes and lysosomal degradation.[36] In 2013, Barna and co-workers reported the screening of 16 antiproliferative compounds against *T. gondii*, two hydrolytically stable ruthenium complexes exhibited 50% inhibitory concentrations of 18.7 and 41.1 nM. To achieve parasiticidal activity with one of them, long-term treatment (22 to 27 days at 80 to 160 nM) was required. Transmission electron microscopy demonstrated ultrastructural alterations of the cells. At 36 h, most *T. gondii* tachyzoites exhibited a completely disorganized cytoplasm, organelles were hardly discernible, and many parasites were embedded in a granular matrix. While these observations indicated a critical metabolic impairment of parasites, the alterations observed do not really point toward a defined mode of action.[37]

The results presented here are in good agreement with those recently reported by us for a diiron(III) compound, which also induced the conversion of the *T. gondii* tachyzoite (active) to the bradyzoite (latent) form. The conversion was noted by the presence of cysts-like structures detected in conventional optical and electron microscopy samples. Beyond cystogenesis, the microscopy images also showed that the treatment induced ultrastructural damages, resulting in the death of a part of the parasite population. These damages include the appearance of structures with myelin-like aspect,

atypical membrane structures on parasite's cytoplasm that are typical of autophagic processes.[20] Here we demonstrated that both compounds reduce the growth of this parasite and also induces the conversion of formation tachyzoite to bradyzoite. Thus, these are promising compounds for the control of this important parasite.

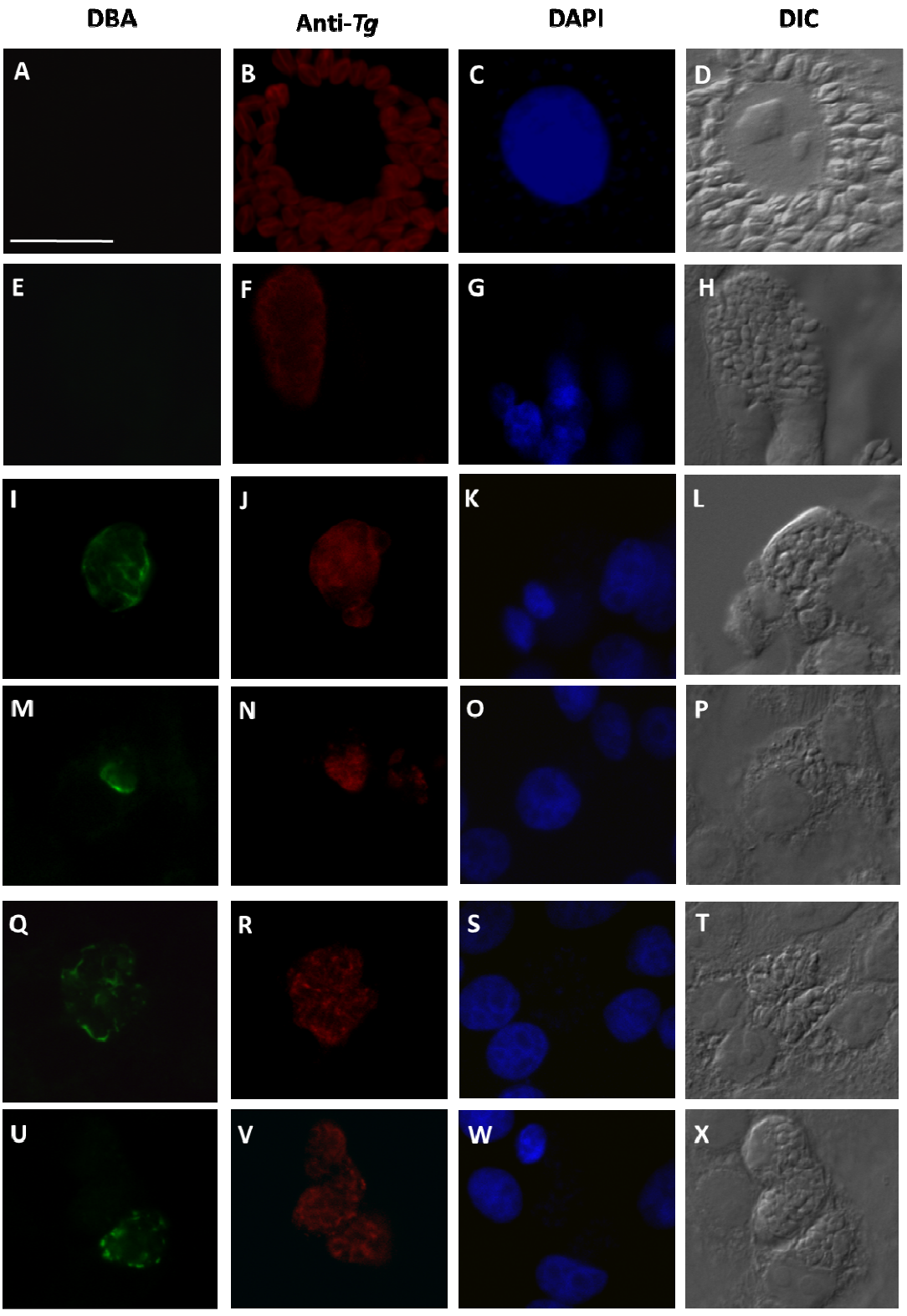

Fig. 7 Fluorescence and differential interferential contrast (DIC) microscopy images of LLC-MK_2 cells infected with tachyzoites of *Toxoplasma gondii* (anti-*Tg*) treated or not with compounds **1**, **2** or sulfadiazine for 48 h labeled with *Dolichos biflorus* (DBA) and

DAPI. A-D. Non-treated cells. E-H. Cells treated with sulfadiazine alone (5 μmol L^{-1}). Cells treated with the compound **1** at 0.5 μmol L^{-1} (I-L) and 5 μmol L^{-1} (M-P). Cells treated with compound **2** at 0.5 μmol L^{-1} (Q-T) and 5 μmol L^{-1} (U-X). Bar = 20 μm.

Unfortunately, they were not able to eradicate the parasite, as desired. However, the findings presented here are of relevance to pave the way in the development of new metal-based anti-toxoplasma drugs for the management of toxoplasmosis, and support the idea that the incorporation of known drugs to metal complexes is an interesting strategy to improve its biological activity.

***In silico* molecular pharmacokinetics properties**

Table 2 presents molecular physicochemical descriptors of the complexes **1**, **2** and sodium sulfadiazine (SDZ). Pharmacokinetics properties were predicted using Molinspiration Cheminformatics server (http://www.molinspiration.com/), which allows us to calculate the octanol-water partition coefficient (LogP), based on group contributions. Properties like molecular hydrophobicity and hydrophilicity, which are involved in drug absorption, bioavailability, hydrophobic drug-receptor interactions, and others properties can also be obtained. The predictions miLogP values of complexes **1**, **2** and sulfadiazine were -6.50, -5.95 and -0.04, respectively. The predictions parameters showed low lipophilicity due to their CLogP value are < 5 (or MLogP is < 4.15), according to the criterion of the Lipinski's Rule of Five, which deals with orally active compounds and defines four simple physicochemical parameter ranges (log P< 5, MW < 500, Hbond acceptors <10 and H-bond donors < 5) associated with 90% of orally active drugs that have achieved phase II clinical status. It is called "Rule of Five" because the border values are 5, 500, 2X5, and 5. [38, 39] These values obtained for logP implie that these complexes have low permeability across cell membrane. Topological Polar Surface Area (TPSA) is a good descriptor used to predict drug absorption,

including intestinal absorption, bioavalibility, Caco-2 permeability and blood brain barrier penetration.[40] The results obtained showed that complex **1** and **2** have higher TPSA values than sulfadiazine: 209.29, 186.36 and 97.98, respectively. Analysis has also shown that a large TPSA (greater than 150-200 $Å^2$) lead to dramatically decreased permeability and oral bioavailability.[41, 42] Hughes et al. observed an increase in adverse events in toxicity studies, *in vivo,* associated with high ClogP value combined with low TPSA < 75 $Å^2$. [42]

The molecular volume is a function of the molecular weight (MW) and shows influence on the transport of molecules and their absorption. In this study, complexes **1** and **2** presented high volume (see Table 2). The number of rotatable bonds (nrotb) is a simple parameter that measures molecular flexibility and is considered a good descriptor of oral bioavailability of drugs. Values beyond 10 lead decreased permeability and oral bioavailability. Complex **1** presents number of rotatable bonds equal 8 while for complex **2** this value is 2, slighty lower than sulfadiazine (Table 3).[43] Complexes **1** and **2** break 3 of the 4 rules, due to inherent features of these compounds like the presence of more than 5 number of hydrogen bonds donors (nOHNH), MW over 500 and more than 10 H-bond acceptors (nON). Aditionally, sulfadiazine did not presented 'n violation' and is orally active drug. These presented violations, strongly related to parameters associated with solubility and permeability, indicate poor permeability and oral bioavailability for compound **1** and **2**. However, there are orally active therapeutic classes outside the 'Rule of Five', as antibiotics, antifungals, vitamins and cardiac glycosides. [44] As mentioned by Lipinski, if a compound fails the Rule of Five, there is a high probability that oral activity problems will be encountered. However, passing the Rule of Five is no guarantee that a compound is drug-like.[38]

Based on the antitoxoplasma activity presented herein, complex **1** is more active than SDZ, however presented 3 violations while SDZ^- pass all the parameteres. Furtermore, the prediction of poor permeability and oral bioavailability exhibited by complex **1** was estimated by *in silico* studies. Both data suggest that complex **1** could be acting by a distinct mode of action than SDZ. In this sense, further studies should be performed in order to understand the mechanism of action of complex **1**, which seems not be trivial. Furthermore, these *in silico* results reported herein will be very useful in the design of future complexes in order to obtain complexes with specific chemical features.

Table 2. Molecular descriptors score for complexes **1** and **2** and sodium sulfadiazine (SDZ).

Compound	miLog P	TPSA	nON	nOHNH	nrotb	n violation	MW	Volume
1	- 6.50	209.29	18	6	8	3	1055.85	829.16
2	-5.95	186.36	13	7	2	3	618.42	450.40
SDZ	-0.04	97.98	6	3	3	0	250.28	202.26

The experimental data indicate that complex **1** have higher activity than complex **2**, which does not presente the ligand HBPA in is structure. Previoulsy, it was stated that this is probably due to the greater lipophilic nature of the complex **1**. However this proposal is not supported by *in silico* results, which indicate poor absorption and permeability across the membrane for complex **1.**

The increased activity of many metal complexes have been explained on the basis of Overtone's concept and the Tweedy´s chelation theory. However, both of them suggest that a high activity is related to a better cell wall permeability and enhancement in the the lipophilicity of the complex,[45,46] what was not found for complexes **1** and **2**. Considering the *in vitro* and *in silico* data it is possible to suggest that the absorption f

complex **1** by the cells may involve a different pathaway than that present by SDZ^-. This may include, for instance, the action of transport protein in the cell wall. This topic will be subject of a new investigation.

Experimental Section

Materials and methods

The CHN elemental analysis for the complexes was performed on a Thermo Scientific FLASH 2000 CHNS/O analyzer. Infrared spectra were recorded with KBr disks on a Shimadzu FT-IR 8300. The electrical conductivity of a $1x10^{-3}$ mol dm^{-3} solution of each complex was measured with a Biocristal conductometer, in DMF. Melting points (MP) were measured on a Microquimica MQAPF-301 apparatus. Full scan mass spectra (MS mode) were obtained on a MicroTOF LC Bruker Daltonics spectrometer equipped with an electrospray source operating in positive ion mode. Samples were dissolved in a MeOH/H_2O (1:1) solution and injected in the apparatus by direct infusion. ^1H and H-H COSY nuclear magnetic ressonance spectra for complexes **1**, **2** and sodium sulfadiazine were obtained on a Bruker Avance 500 MHz spectrometer in deuterated dimethyl sulfoxide (d6-DMSO).

Synthesis and characterization of the zinc complexes [(SDZ)Zn(μ-BPA)$_2$Zn(SDZ)] **1** and [Zn(SDZ)(HSDZ)(Cl)(OH_2)] **2**

Complex **1** was obtained by the addition of an aqueous solution of NaSDZ to a methanolic solution of [Zn(HBPA)Cl_2],[21] under stirring, which resulted in the precipitation of a beige solid. The complex was recrystallized in acetonitrile:water (1:1) resulting in suitable crystals for crystallographic analysis. Yield: (214 mg, 38%). Anal. Calc. for $C_{46}H_{52}N_{12}O_{10}S_2Zn_2$ (FW 1127.86): C, 49.04; H, 4.56; N, 14.68. Found: C,

48.99; H, 4.65; N, 14.90%. IR cm^{-1}: 3356 and 3423 (NH_2), 3039 (CH aromatic), 1595 (C=N), 1442 (C=C), 1341 and 1157 (SO_2), 769 (CH aromatic). Mp. 189 °C. ΛM (DMSO)= 8 Ω^{-1} cm^2 mol^{-1} (no electrolyte type).

Complex **2** was obtained by the reaction between $ZnCl_2$ and NaSDZ, under the same conditions described for complex **1**, which resulted in a white solid. The solid was recrystallized in acetonitrile:water (1:1) resulting in a microcrystalline white solid. Yield: (110 mg, 18%).Anal. Calc. $C_{20}H_{21}N_8O_5S_2ZnCl$ (FW 618.39): C, 38.85; H, 3.42; N, 18.12. Found: C, 38.86; H, 3.41; N, 17.97%.IR cm^{-1}: 3354 and 3424 (NH_2), 3038 (CH aromatic), 1593 (C=N), 1442 (C=C), 1328 and 1157 (SO_2), 769 (CH aromatic). Mp. 233°C. ΛM (DMSO)= 4 Ω^{-1} cm^2 mol^{-1} (no electrolyte type).

Crystal data collection and refinement

Crystallographic analysis of the complex **1** was made from a selected block cut off from a big single crystal separated from the homogeneous crystalline sample. X-ray diffraction data were measured on a Bruker Kappa APEX II Duo diffractometer using Mo sealed tube (1.5 KW) and the temperature of the sample was set at 173 K with Oxford Cryostream 700 series system. Intensities were collected with ω and ϕ scans and were corrected for Lorentz and polarization effects and for absorption (multi-scan).

[47, 48]A conformational disorder was modeled for N1 and C10 atoms with two alternative positions and with refined occupancy factor of 0.692(14) and 0.308(14). One water solvate is also disordered and in this case the occupation factors for oxygen atom are distributed over 4 alternative positions with site occupancy of 0.40, 0.25, 0.20 and 0.15. N1 and C10 atoms are disordered over two alternative positions with refined occupancy factor of 0.692(14) and 0.308(14) and the hydrogen atom of the disordered amine group was not located from Difference Fourier Map. Restraints were applied to four carbon

atoms of the pyridine (C43/C46) due to high vibrational motion observed in this ring. The restraints were applied with ISOR, SIMU and DELU instructions. All non-hydrogen atoms were refined with anisotropic displacement parameters. Hydrogen atoms bonded to C atoms were placed at their idealized positions using standard geometric criteria. H atoms of the water solvate were located from Fourier difference maps, except for disordered molecule, and treated with riding model. Checking procedure of the final refinement and ORTEP picture were performed with PLATON software.[49] Crystallographic and structure refinement data for complex **1** are shown in Table 3.

Table 3. Crystal data and structure refinement for compound **1**.

Empirical formula	$C_{46}H_{52}N_{12}O_{10}S_2Zn_2$
Formula weight	1127.86
Temperature	173(2) K
Wavelength	0.71073 Å
Crystal system	Orthorhombic
Space group	Pbca
Unit cell dimensions	a = 14.6884(3) Å
	b = 20.5485(5) Å
	c = 32.5555(8) Å
Volume	9826.1(4) $Å^3$
Z	8
Density (calculated)	1.525 Mg/m^3
Absorption coefficient	1.132 mm^{-1}
F(000)	4672
Crystal size	0.40 x 0.24 x 0.18 mm^3
Theta range for data collection	1.87 to 32.12°
Index ranges	$-20 \le h \le 21$, $-29 \le k \le 30$, $-46 \le l \le 48$
Reflections collected	103708
Independent reflections	17171 (R_{int} = 0.0348)
Absorption correction	Semi-empirical from equivalents
Max. and min. transmission	0.8222 and 0.6602

Refinement method	Full-matrix least-squares on F^2
Data / restraints / parameters	17171 / 47 / 695
Goodness-of-fit on F^2	1.148
Final R indices [I>2σ(I)]	R1 = 0.0480, wR2 = 0.1139
R indices (all data)	R1 = 0.0628, wR2 = 0.1218
Largest diff. peak and hole	0.817 and -0.818 e.$Å^{-3}$

In vitro investigation of anti-toxoplasma activity

Toxoplasma gondii

Tachyzoites from RH strain were maintained by intraperitonial passages every 2-3 days in Swiss mice. The parasites were obtained by peritoneal lavage with phosphate buffered saline (PBS) and centrifuged at 500 g for 10 min at 4°C. The collected parasites were ressuspended in DMEM and counted in a Neubauer chamber. This work was performed in accordance with the animal experimentation Brazilian Law #11794/08. The protocol was approved by the Committee on the Ethics of Animal Experiments of the *Universidade Estadual do Norte Fluminense Darcy Ribeiro* (Permit Number: 259).

Culture of LLC-MK_2 cells

The LLC-MK_2 cells (epithelial kidney cells from *rhesus monkey*) were maintained in 25 cm^2 culture flasks with Dulbecco´s modified Eagle´s medium (DMEM) supplemented with 5% fetal bovine serum (FBS). For infection, cells cultured in flasks were seeded over coverslips in 24-well culture plates at 2 x 10^5 cells per well. After 24 h, the cells were infected with 1 x 10^6 *T. gondii* per well and treated with the compounds at different concentrations for 24 and 48 h (see below).

Cell viability assays

The possible toxic effects of the compounds **(1)** and **(2)** to the host cell were evaluated by the reduction of 3-(4,5-dimethylthiazol-2-yl)-2,5-diphenyltetrazolium bromide (MTT) by live cells. For these assays, 1 x 10^5 cells were seeded per well in 96-well culture plates with 200 µL of DMEM supplemented with 5% FBS for 24 h. After 2 h, cells were treated with the compounds at concentration from 100 to 0.2 µmol.L^{-1} derived from a serial dilution in DMEM supplemented with 5% FBS. For positive control, cells were cultured in DMEM supplemented with 5% FBS only, and for negative control, cells were cultured in the presence of 10% Triton X-100 in PBS. After treatment, 50 µL of the culture supernatant was removed and 15 µL of MTT solution (5 mg/ml) in PBS was added to each well for 3 h. The formazan crystals were solubilized with 100 µL of pure DMSO. The plate was centrifuged at 400 g for 10 min, 100 µL of the supernatant was collected, transferred to a new 96-well plate that was read at 570 nm in a Versamax microplate reader (Molecular Devices) using the 6.0 SoftMax Pro®. Data shown are representative of three independent experiments.

Anti-proliferative assays

After 24 h of seeding, the LLC-MK2 cells were washed, infected with a 5:1 parasite: host cell ratio for 1 h at 37°C. The cells were washed with Hank's solution to remove extracellular parasites. DMEM supplemented with 5% FBS containing compexes **1** or **2** at concentration of 0.5, 1.0 and 5.0 µmol L^{-1} were added to the cells. After 24 and 48 h of treatment, the cells were fixed with 4% formaldehyde in PBS solution, stained with Giemsa, dehydrated in different concentrations of acetone-xylene and observed under an optical microscope Zeiss Axioplan. At least 200 host cells for each coverslips, on three different coverslips per experiment, were counted and the infection index was calculated by multiplying the "mean number of internalized *T. gondii* per host cell" by

the "percentage of infected host cells". The data were plotted in Microsoft Excel 2013 and statistically analyzed by using the GraphPad PRISM® 5 by *two-way* ANOVA.

Fluorescence microscopy

Cells infected with parasites, untreated or treated with complexes **1**, **2** or NaSDZ were washed once with Hank's solution, fixed with 3% formaldehyde in PBS for 1 h and permeabilized with 0.5% Triton X-100 in PBS for 10 min. Cells were washed with PBS, incubated with 100 mmol L^{-1} of ammonium chloride in PBS for 30 min and washed with 3% bovine serum albumin in PBS (BSA-PBS). The cells were incubated with antitoxoplasma antibody (1:4000 in BSA-PBS) for 1 h. Subsequently cells were washed with BSA-PBS and incubated with *Dolichos biflorus* lectin-FITC (Sigma) (1:400 in BSA-PBS) for 1 h, washed, incubated with anti-mouse antibody conjugated with TRICT (1:400 in BSA-PBS) for 1 h at room temperature. The coverslips were washed, mounted with Prolong Gold with DAPI and observed in a Zeiss Axioplan microscope equipped with differential interference contrast microscopy, 100 HBO mercury lamp, and the images were captured with a AxioCam MRC5 digital camera with the Zeiss Axiovision system and processed with Adobe Photoshop 6.0.

Calculation of Molecular Physicochemical Properties

Structures of the complex were drawn by using ACD/ChemSketch for academic and personal use and their MDL Molfiles were generated. Then, the structures were pasted to online Molinspiration Cheminformatics 2015 version 2014.11 server (www.molinspiration.com) for calculation of molecular physicochemical properties, such as, miLogP, Topological Polar Surface Area (TPSA), Molecular Weight (MW),

number of hydrogen bonds donors (nOHNH) and acceptors (nON), number of atoms, number of rotatable bonds, Volume, n Violation (number of Rule of 5 violations). For calculations, the option "Calculate Properties" was selected and the properties predictions were calculated.

Conclusions

Complexes **1** and **2** reduced the growth of *T. gondii* in LLC-MK2 cells and they were non-toxic to the host cells. Complex **1** presented the most effective anti-toxoplasma activity, reducing the growth of *T. gondii* after 24 and 48 h of treatment. Complex **2** was not active after 24 h of treatment but presented similar results to those shown by the compound **1** after 48 h of treatment. After 48 h of incubation with both compounds, the parasites were clusters and edges of the parasitophorous vacuoles were highly stained suggesting the formation of pseudocysts that were confirmed by DBA labeling. The presence of these pseudocysts indicates that both compounds promoted conversion of tachyzoites to bradyzoites. Results obtained by *in silico* studies showed that complexes **1** and **2** present lower absorption and permeability than sulfadizine. However, these complexes showed higher efficacy than sulfadizine. Further investigations will be carried out aiming to clarify the mechanism of action of both complexes which seem to differ from that presented by SDZ, since complex **1** showed higher antitoxoplasma activity than SDZ.

Acknowledgements

The authors are grateful to financial support received from CAPES (Coordenação de Aperfeiçoamento de Pessoal de Nível Superior), CNPq (Conselho Nacional de Desenvolvimento Científico e Tecnológico), FAPERJ (Fundação Carlos Chagas de

Amparo à Pesquisa do Estado do Rio de Janeiro) and FINEP (Financiadora de Estudos e Projetos).

Appendix A. Supplementary material

Full crystallographic tables (including structure factors) for complex **1** have been deposited with the Cambridge Crystallographic Data Centre as supplementary publication number CCDC 1410012. These data can be obtained free of charge from The Cambridge Crystallographic Data Centre via www.ccdc.cam.ac.uk/data_request/cif.

References

[1] F. Robert-Gangneux and M. L. Dardé, *Clin. Microbiol. Rev.,* 2012, **25**, 264.

[2] M. S. Ferreira and A. S. Borges, *Mem. Inst. Oswaldo. Cruz.,* 2002, **97**, 443.

[3] C. Paquet and M. H. Yudin, J. *Obstet. Gynaecol. Can.,* 2013, **35**,78.

[4] K. D. C. Jensen, A. Camejo, M. B. Melo, C. Cordeiro, L. Julien, G. M. Grotenbreg, E. Frickel, H. L. Ploegh, L. Young and J. P. J. Saeija, *mBio.,* 2015, **6**, 1.

[5] A. J. A. M. van der Ven, E. M. E. Schoondermark-van de Ven, W. Camps, W. J. G. Melchers, P. P. Koopmans, J. W. M. van der Meer and J. M. D. Galama, *J. Antimicrob. Chemother.,* 1996, **38**, 75.

[6] C. Silveira, R. Belfort, C. Muccioli, G. N. Holland, C. G. Victora, B. L. Horta, Y. Fei and R. B, Nussenblatt, *Am. J. Ophthalmol.,* 2002, **134**, 41.

[7] A. Yazici, P. C. Ozdal, I. Taskintuna, S. Kavuncu and G. Koklu, *Ocul. Immunol. Inflamm.,* 2009, **17**, 289.

[8] S. Kongsaengdao, K. Samintarapanya, K. Oranratnachai, W. Prapakarn and C. Apichartpiyakul, *J. Int. Assoc.Physicians AIDS Care.,* 2008, **7**,11.

[9] R. R. Coombs, M. K. Ringer, J. M. Blacquiere, J. C. Smith, J. S. Neilsen, Y.-S. Uh, J. B. Gilbert, L. J. Leger, H. Zhang, A. M. Irving, S. L. Wheaton, C. M. Vogels and S. A. Westcott, *Transition Met. Chem.,* 2005, **30**, 411.

[10] J. P. F. Felix, R. P. C. Lira, R. S. Zacchia, J. M. Toribio, M. A. Nascimento and C. E. L. Arieta, *Am. J. Ophthalmol.,* 2014, **157**, 762.

[11] O. Megged, I. Shalit, I. Yaniv, J. Stein, S. Fisher and I. Levy, *Pediatr. Transplant.,* 2008, **12**, 902.

[12] A. Reis, C. Valmaggia, T. Tandogan, K. Rippe and O. Girmann, *J. Clin. Exp. Ophthalmol.,* 2015, **6**, 1.

[13] S. Rajapakse, C. Shivanthan , N. Samaranayake, C. Rodrigo and F. S, Deepika, *Pathog Glob Health.,* 2012, **107**,162.

[14] M. Harell and D. E. Carvounis. *J. Ophthalmol.,* 2014, **2014**. doi: 10.1155/2014/273506

[15] E. Kamau, T. Meehan, M. D. Lavine, G. Arrizabalaga, G. M. Wilson and J. Boyle, *Antimicrob. Agents Chemother.,* 2011, **55**, 5438.

[16] A.Horn Jr, G. L. Parrilha, K. V. Melo, C. Fernandes, M. Horner, L. C. Visentin, J. A. S. Santos, M. S. Santos, E. C. A. Eleutherio and M. D. Pereira, *Inorg. Chem.,* 2010, **49**, 1274.

[17] C. Fernandes, R. O. Moreira, L. M. Lube, A. Horn Jr., B, Szpoganicz, S. Sherrod and D. H. Russell, *Dalton Trans.,* 2010, **39**, 5094.

[18] A. Horn Jr, C. Fernandes, G. L. Parrilha, M. M. Kanashiro, F. V. Borges, E. J T. de Melo, G. Schenk, H. Terenzi and C. T. Pich*, J. Inorg. Biochem.,* 2013, **128**, 38.

[19] T. P. Ribeiro, C. Fernandes, K. V. Melo, S. S. Ferreira, J. A. Lessa, R. W. A. Franco, G. Schenk, M. D. Pereira and A. Horn Jr., *Free Radic. Biol. Med.,* 2015, **80**, 67.

[20] J. A. Portes, T. Souza, T, Santos, L. Silva, T. Ribeiro, M. D. Pereira, A. Horn Jr, C. Fernandes, R. A. DaMatta, W. Souza and S. H. Seabra, *Antimicrob. Agents Chemother.,* in press.

[21] C. Fernandes, A. Horn Jr., O. Vieira-da-Motta, M. M. Kanashiro, M. R. Rocha, R. O. Moreira, S. R. Morcelli, B. F. Lopes, L. da S. Mathias, F. V. Borges, L. J. H. Borges, L. C. Visentin and J. C. de A. Almeida, *Inorg. Chim. Acta.,* 2014, **416**, 35.

[22] A. M. Avunduk, M. C. Avunduk, A. K. Baltaci and C. A. Mustafa. *Ophthalmologica.,* 2007, **221**, 421.

[23] G. Seyoum and T. V. Persuad, *Histopathol.,* 1995, **10**, 25.

[24] E. Mocchegiani, R. Giacconi, M. Muzzioli and C. Cipriano, *Mech. Ageing. Dev.,* 2000, **121**, 21.

[25] K. R. Grünwald, M. Volpe and N. C. Mösch-Zanetti*, J. Coord. Chem.,* 2012, **65**, 2008.

[26] G. Marinescu, G. Marin, A. M. Madalan, A. Vezeanu, C. Tiseanu, and M. Andruh., *Cryst. Growth Des.*, 2010, **10**, 2096.

[27] J. Chen, X. Wang, Y. Zhu, J. Lin, X. Yang, Y. Li,Y. Lu and Z. Guo, *Inorg. Chem.,* 2005, **44**, 3422.

[28] K. Selmeczi, C. Michel, A. Milet, I. Gaultier-Luneau, C. Philouze, J. L. Pierre, D. Schnieders, A. Rompel and C. Belle., *Chem. Eur. J.*, 2007, **13**, 9093.

[29] A. Horn Jr, L. Fim, A. J. Bortoluzzi, B. Szpoganicz, M. de S. Silva, M. A. Novak, M. B. Neto, L. S. Eberlin, R. R. Catharino, M. N. Eberlin and C. Fernandes, *J. Mol. Struct.,* 2006, **797**, 154.

[30] N. C. Baenziger, S.L. Modak and C. L. Fox Jnr, *Acta Cryst.,* 1983, **C39**, 1623.

[31] R.-X. Yuan, R.-G. Xiong, Z.-F. Chen, P. Zhang, H.-X. Ju, Z. Dai, Z.-J. Guo, H.-K. Fun and X.-Z. You, *J. Chem. Soc. Dalton Trans.***,** 2001, **6**, 774.

[32] J. Guo, L. Li, Y. Ti and J. Zhu, *eXPRESS Polymer Letters.,* 2007, **1**, 166.

[33] G. Huschek, D. Hollmann, N. Kurowski, M. Kaupenjohann and H. Vereecken, *Chemosphere.,* 2008, **72(10)**, 1448.

[34] G. M. G. Hossain, A.J. Amoroso, A. Banu and K.M.A. Malik, *Polyhedron.,* 2007, **26**, 967.

[35] J. A. Portes, C. D. Netto, A. J. M. Da Silva, P. R. R. Costa, R. A, DaMatta, T. A. T. Dos Santos, W. De Souza and S. H. Seabra, *Veterinary Parasitology,* 2012, **186**, 261.

[36] Y. M. Ling, M. H. Shaw, C. Ayala, I. Coppens, G. A.Taylor, D. J.Ferguson et al, *J. Exp. Med.,* 2006, **203**, 2063.

[37] F. Barna, K. Debache, C. A. Vock, T. Küster and A. Hemphilla, *Antimicrob. Agents Chemother.,* 2013, **57(11)**, 574.

[38] C. A. Lipinski, *Drug Discovery Today: Technology.,*2014, **11**.

[39] C.A. Lipinski, F. Lombardo, B.W. Dominy and P.J. Feeney, *Adv.Drug.Deliv. Rev.* 1997, **23**, 3.

[40] N. K. Borra and Y. Kuna. *Int. J. Pure App. Biosci.,* 2013**, 1(4)**, 28.

[41] D.E. Clark. *J. Pharm. Sci.,* 2000, **88**, 807.

[42] J. D. Hughes, J. Blagg, D. A. Price et al, *Bioorg. Med. Chem. Lett.,* 2008, **18(17)**, 4872.

[43] D. F. Veber, S. R. Johnson, H. Y. Cheng HY et al, *J. Med. Chem.,* 2002, **45**, 2615.

[44] C. A. Lipinski, F. Lombardo, B. W. Dominy and P. J. Feeney, *Adv. Drug Deliv.Rev,.* 2012, **64**, 4.

[45] Y. Anjaneyulu and R.P. Rao, *Synth. React. Inorg. Met-Org. Chem.,*1986, **16**, 257.

[46] A. A. Al-Amiery, A. A. H. Kadhum and A. B. Mohamad., *Bioinorg. Chem. and Applic.,* 2012, **2012**. doi:10.1155/2012/795812.

[47] Bruker APEX2, SAINT and SADABS, version 2011.8-0; Bruker AXS Inc., Madison, Wisconsin, USA.

[48] G. M. Sheldrick, *Acta Cryst. A.,* 2008, **64**, 112.

[49] A. L. Spek, *Acta Cryst. D.,* 2009, **65**,148.

Graphical Abstract